Available online at www.sciencedirect.com
ScienceDirect
Trans. Nonferrous Met. Soc. China 32(2022) 4041−4049
Transactions of Nonferrous Metals Society of China
www.tnmsc.cn

3D MoS_2/graphene nanoflowers as anode for advanced lithium-ion batteries

Han-bing HE[1], Zhen LIU[1], Chao-qun PENG[2], Jun LIU[2], Xiao-feng WANG[2], Jing ZENG[1]

1. School of Metallurgy and Environment, Central South University, Changsha 410083, China;
2. School of Materials Science and Engineering, Central South University, Changsha 410083, China

Received 27 July 2021; accepted 27 April 2022

Abstract: Vertical MoS_2 nanosheets were controllably patterned onto graphene as nanoflowers through a two-step hydrothermal method. The interconnected network and intimate contact between MoS_2 nanosheets and graphene by vertical channels enabled a high mechanical integrity of electrode and cycling stability. In particular, MoS_2/graphene nanoflowers anode delivered an ultrahigh specific capacity of 901.8 mA·h/g after 700 stable cycles at 1000 mA/g and a corresponding capacity retention as 98.9% from the second cycle onwards.
Key words: MoS_2; graphene; 3D nanoflowers; nanosheets; lithium-ion batteries

1 Introduction

There is an urgent requirement for sustainable development of new energy accompanying the global warming and energy crisis [1]. The demand for high-power vehicles and smart grid arises the rapid evolution of lithium-ion batteries. With the appearance of monolayer graphene, a variety of two-dimensional (2D) materials, such as transition metal dichalcogenides (TMDs) [2,3], transition metal oxides (TMOs) [4,5] and transition metal carbide and nitrides (MXenes) [6,7] nanosheets, are once again on the horizon as its structure analogues.

Molybdenum disulfide (MoS_2), one of the most important members of TMDs, has attracted much attention because of its graphene-like lamellar structure [8]. Recently, layered MoS_2 has become the potential candidate for anode material of lithium-ion batteries due to the higher theoretical specific capacity (670 mA·h/g) compared with the conventional graphite anode (372 mA·h/g), and the large theoretical interspacing (0.615 nm), which creates favorable conditions for Li^+ insertion and desertion [9]. However, the poor electronic/ionic conductivity and rapid capacity fading limit its practical applications. At the same time, the intermediate product Li_2S of the transformation reaction is easy to react with the electrolyte to form a thick gel-like polymer layer, which will inhibit the reaction and damage the cyclic stability and rate performance of the active material [10].

Reducing the number of MoS_2 layers or increasing their lamellar spacing is often used to overcome these issues. Designing novel hybrid nanostructures has been an alternative way by integrating diverse functionalities into a single system [11,12]. Extensive research has proven that the combination of graphene and its derivatives can improve the conductivity and stability of the entire hybrid, due to the high electrical conductivity and excellent structure stability of graphene [9,13,14]. For example, WANG et al [15] reported that vertically aligned MoS_2 nanosheets patterned on

Corresponding author: Jing ZENG, Tel: +86-15116335400, E-mail: zengjing@csu.edu.cn;
Xiao-feng WANG, Tel: +86-13467516329, E-mail: wangxiaofeng@csu.edu.cn
DOI: 10.1016/S1003-6326(22)66076-X

electrochemically exfoliated graphene (EG) and the prepared anode delivered an ultrahigh-specific capacity of 1250 mA·h/g after 150 cycles at 1 A/g. Although a large number of hybrids (MoS_2/graphene nanosheets [16], MoS_2/N-doped grapheme [17], 3D MoS_2/grapheme [18]) have been developed recently, these hybrids were not well controlled in structure, hindering further development of MoS_2-based composites for high-performance energy storage. This would result from the fact that the anticipated advantages of graphene in grapheme/MoS_2 composite were not fully exerted and can be solved by developing new grapheme/MoS_2 hybrid nanostructures.

In this work, flower-like MoS_2 with nanosheets on the surface of graphene was designed as 3D MoS_2/graphene nanoflowers via solvothermal and hydrothermal methods. The flower-like MoS_2 vertical nanosheets is conducive to the penetration of electrolyte and can shorten the diffusion distance of Li^+, and 3D conducting graphene networks also enhance the electrical conductivity of the whole electrode.

2 Experimental

2.1 Preparation of MoO_2/graphene composite

MoO_2/graphene composite was prepared according to our previous literature [19]. In detail, 0.3 g commercial MoO_3 was added into the mixture of 10 mL ethylene glycol, 3 mL grapheme oxide (GO) suspension (10 mg/mL) and 30 mL distilled water under continuous stirring. Then, the mixture was transferred into a 50 mL Teflon-lined stainless-steel autoclave and kept at 180 °C for 12 h. The sample was collected after washing by deionized water and ethanol, as well as drying in vacuum overnight. Finally, the dark MoO_2/graphene composites were obtained through heat treatment at 500 °C for 2 h in 5%H_2/Ar atmosphere.

2.2 Preparation of MoS_2/graphene nanoflowers

1 mmol MoO_2/graphene composite, 2 mmol $Na_2S·9H_2O$ and 15 mL distilled water were mixed and stirred for 30 min. And then 10 mL HCl solution was added into the mixture. The mixture was stirred for another 10 min and transferred into a 50 mL Teflon-lined stainless-steel autoclave and kept at 230 °C for 6 h. The MoS_2/graphene nanoflowers were collected after washing by distilled water and ethanol and drying at 60 °C. The schematic diagram of the synthesis process for MoS_2/graphene nanoflowers is shown in Fig. 1.

2.3 Materials characterization

X-ray diffraction (XRD) patterns were obtained on a Rigaku D/max 2500 using Cu K_α radiation (λ=0.15405 nm) scanning in a range of 10°−80° at a sweep speed of 8 (°)/min. Raman spectroscopy was detected using a LabRAM HR 800 Raman spectrometer (HORIBA Jobin Yvon, France) in a scanning range of 100−500 cm^{-1}. The surface and cross-section morphologies were determined using a scanning electron microscope (SEM, Nano SEM 230, FEI, America). Thermal gravimetric analysis (TGA, STA449F3, NETZSCH, Germany) was used to detect the content of every component with a heating rate of 10 (°)/min in air. And the crystal structures of micro-sized composite were collected using a transmission electron microscope (TEM, Tecnai G2 F20, FEI, America).

2.4 Electrochemical tests

CR2016 coin cells were assembled and used for the electrochemical experiment. The MoS_2/graphene nanoflowers, acetylene black, and polyvinylidene fluoride (PVDF) were used as active material, conductive agent, and binder at a mass ratio of 7:2:1. Then, the slurry was pasted on a copper foil and dried in a vacuum oven at 110 °C for 12 h. The electrolyte consists of ethylene

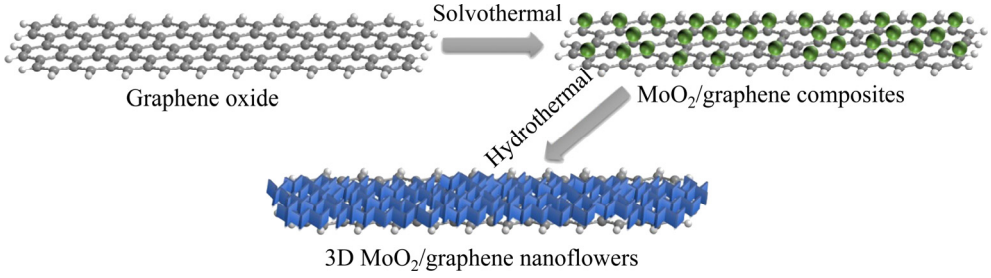

Fig. 1 Schematic illustration of formation process for MoS_2/graphene nanoflowers

carbonate (EC)/diethyl carbonate (DEC)/dimethyl carbonate (DMC) (volume ratio 1:1:1) with 1 mol/L $LiPF_6$. The electrode performance was characterized by cyclic voltammetry (CV) and galvanostatic charge−discharge (GCD). These tests were performed on an electrochemical workstation (CHI604E and IM6ex, China) and a Land automatic battery tester (Wuhan, China). The test parameters were as follows, in regard of galvanostatic charge−discharge, $\varphi_{initial}$=3.0 V, φ_{end}=0.01 V (vs Li/Li^+), with respect to CV, voltage=0.01−3.0 V (vs Li/Li^+), scan rate=0.1 mV/s.

3 Results and discussion

3.1 Phase structure and chemical component analysis

The crystal structure of as-obtained MoO_2/graphene composites and MoS_2/graphene nanoflowers are shown in Fig. 2(a). In the XRD pattern of MoO_2/graphene composites, the characteristic peaks located at 2θ=26°, 37° and 53.5° are well indexed to the (001), ($\bar{2}$11) and ($\bar{3}$11) planes of MoO_2 (monoclinic, JCPDS: 65-5787), respectively. As for MoS_2/graphene nanoflowers, the dominant characteristic peaks located at 2θ=13.8°, 33.2°, 39.5° and 58.9° are well indexed to the (002), (110), (103) and (110) planes of 2H-MoS_2 (hexagonal, JCPDS: 37-1492). No redundant peaks of other phases are detected, indicating that the purity of sample is very high. The widths of those peaks are narrow, suggesting that both composites are fine-grained. Besides, the theoretical 2θ corresponding to (002) plane in the standard PDF card of MoS_2 is 14.4°, with an interplanar spacing as 0.63 nm [20]. However, the experiment value of 2θ is 13.8°, meaning a higher interplanar spacing as 0.65 nm, which is benefit for the insertion and extraction of Li^+. Furthermore, Raman tests were carried out to confirm the existence of carbon, as shown in Fig. 2(b). The broad peaks at 1350 and 1580 cm^{-1} are characteristic features of carbon. The intensity ratio of D-band to G-band (I_D/I_G) is large than 1, showing the partially graphitizing of the carbon matrix, which could improve the electron transportation of both composites. The carbon content in the MoS_2/graphene nanoflowers was determined by TGA as shown in Fig. 2(c), which was calculated to be about 19.5 wt.%.

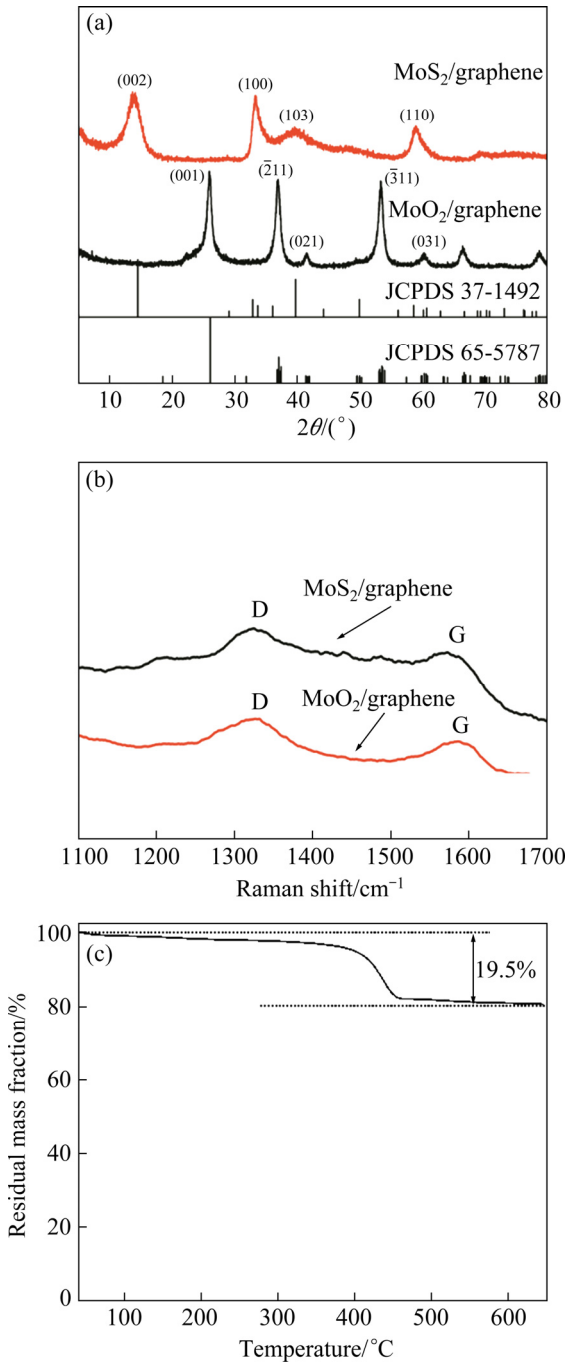

Fig. 2 XRD patterns (a) and Raman spectra (b) of MoO_2/graphene composites and MoS_2/graphene nanoflowers, and TGA curve of MoS_2/graphene nanoflowers heated at 10 °C/min in air atmosphere (c)

3.2 Morphology and microstructure

SEM and TEM images are characterized to obtain the morphology and structure of the MoO_2/graphene composites and MoS_2/graphene nanoflowers in Fig. 3. The particles of MoO_2 are very fine (5−10 nm) and evenly dispersed in MoO_2/graphene composites (Fig. 3(a)). The ultrafine MoO_2 nanoparticles grow on the surface

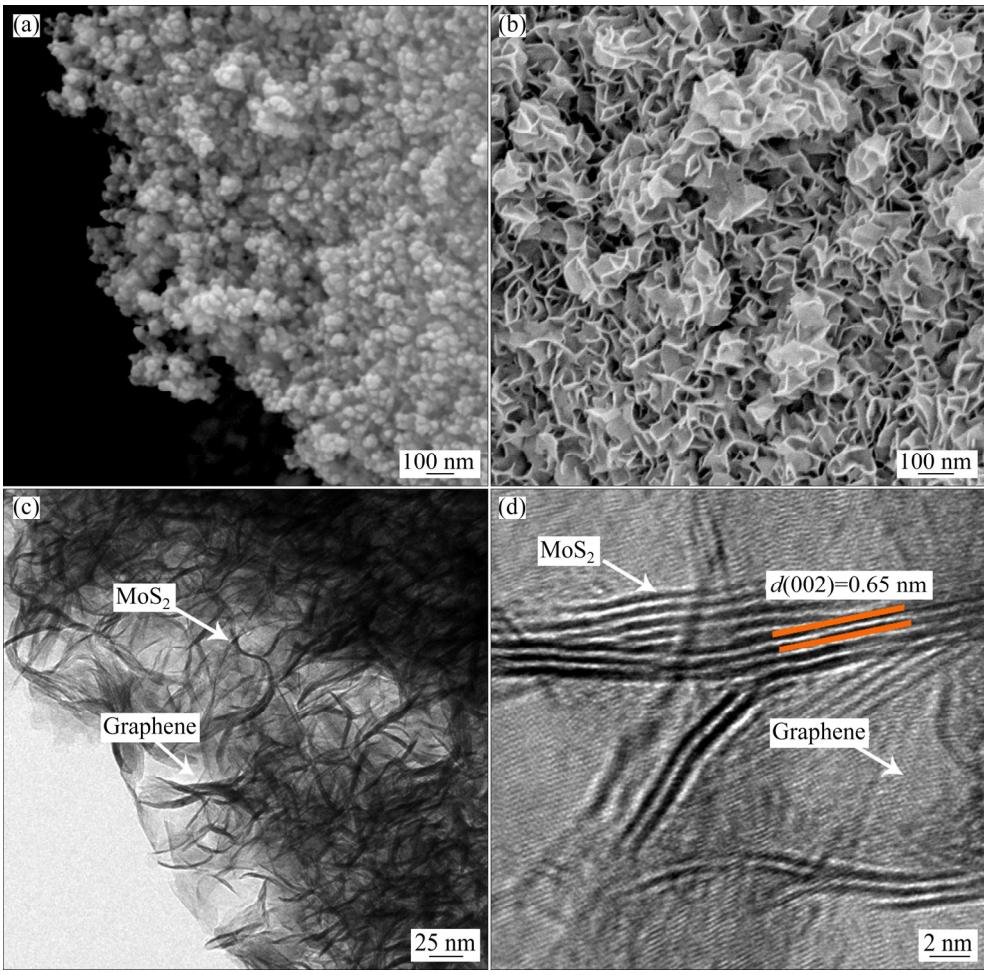

Fig. 3 SEM images of MoO_2/graphene (a) and MoS_2/graphene nanocomposite (b), and TEM (c) and HRTEM (d) images of MoS_2/graphene nanoflowers

of the graphene, in return the graphene tightly covers the surface of the active material. After sulfidation, MoO_2/graphene composites change into 3D MoS_2/graphene nanoflowers as shown in Fig. 3(b). Plenty of MoS_2 nanoflowers with an average size of 150−250 nm pattern closely and uniformly on the graphene substrate, forming a whole piece of huge nanoflowers. The vertical MoS_2 nanosheets, which connected with each other through local cross contact instead of overlapping, are controllably patterned onto graphene as nanoflowers. MoS_2 nanoflowers were packed tightly onto the graphene sheets, which is benefit for the diffusion of Li^+, and also improving the contact area of active materials and electrolyte. As shown in Fig. 3(c), the transparent and curly MoS_2 nanosheet with thickness of 3−6 nm is growing on the graphene substrate, which is consistent with Fig. 3(b). Figure 3(d) shows the HRTEM of MoS_2/graphene nanoflowers, which further clarifies that the MoS_2 nanoflowers are lamellar structure consisting of several layers stacked on top of each other. In addition, the interlayer space is 0.65 nm, which corresponds to the specific (002) surface of the orthorhombic MoS_2.

TEM image and corresponding EDS patterns (Fig. 4) illustrate that Mo, S and C elements are homogeneously distributed in MoS_2/graphene nanoflowers, which proves the presence of graphene. Graphene enhances the electrical conductivity of the material and makes the structure more stable.

3.3 Electrochemical performance

To further explore the structural advantages of the MoS_2/graphene nanoflowers as an alternative electrode material of lithium-ion batteries, electrochemical tests were conducted. Figure 5(a) displays

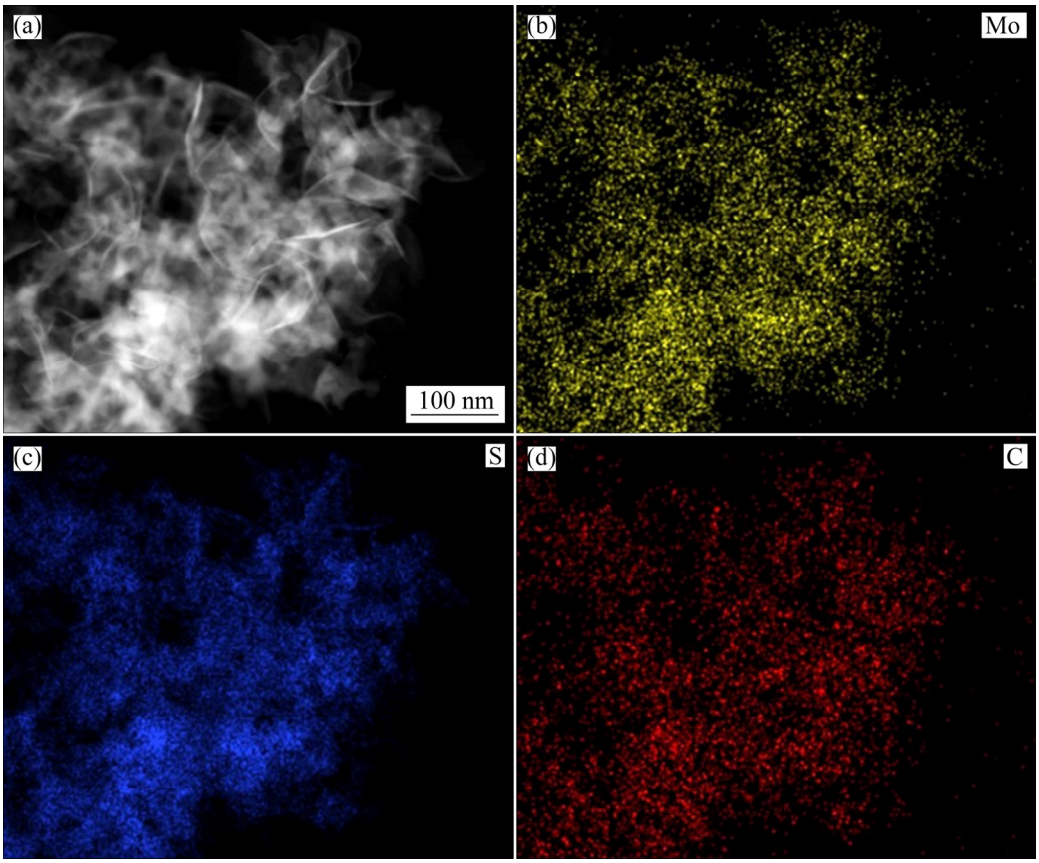

Fig. 4 TEM image (a) and corresponding EDS mappings (b, c, d) of MoS_2/graphene nanoflowers

the CV spectra of the first three cycles of the MoS_2/graphene nanoflowers at a scan rate of 0.1 mV/s in a range of 0−3 V (vs Li/Li^+), respectively. The two reduction peaks at 0.4 and 1.4 V in the first cathodic scan can be detected. The former is attributed to the reaction of $Li_xMoS_2+(4-x)Li^++(4-x)e\rightarrow Mo+2Li_2S$ and the forming of SEI film, resulting in the capacity loss. The latter is owing to the reaction of Li^+ embedding MoS_2 to form Li_xMoS_2 and the transformation of MoS_2 from 2H (tri-prism) to 1T (octahedron). The first anode scan only has two obvious oxidation peaks located at 1.7 and 2.3 V, respectively, which are related to the partial oxidation of Mo to form MoS_2, the desulfurization process of Li_2S and the formation of S. In the subsequent discharge, the peak at 0.4 V disappears and that at 1.4 V is reinforced as well as the peak at 1.9 V appears. The first two is caused by the combination of Mo and Li, the 3rd one shows the formation of Li_2S. The overlapping of next two cycles indicates the remarkable reversibility of MoS_2/graphene anode.

In order to study the cyclic properties of MoS_2/graphene anode, the galvanostatic charge−discharge curves are tested from the 1st to 100th cycles at the current density of 100 mA/g as shown in Fig. 5(b). The initial discharge capacity of the MoS_2/graphene anode is 1460 mA·h/g and corresponding coulombic efficiency is 57.9%, which is related to the formation of SEI film and decomposition of electrolyte. From the 5th cycle onwards, the coulombic efficiencies stay above 98% and from the 2nd cycle onwards, the capacity retention is 91.1% after 100 cycles. For comparison, the galvanostatic charge−discharge curves of pure MoS_2 anode are also presented in Fig. 5(c). The initial discharge capacity of the pure MoS_2 anode is 338.1 mA·h/g and corresponding coulombic efficiency is 69.6%. With the increase of cycle number, the specific capacity of pure MoS_2 anode first increases over 800 mA·h/g and then quickly fades to 256 mA·h/g after 75 cycles. Meanwhile, charge−discharge profiles of MoS_2/graphene anode in the first three cycles are also illustrated under the same conditions as shown in Fig. 5(d). The voltage platform at about 0.5 and 1.0 V of the first

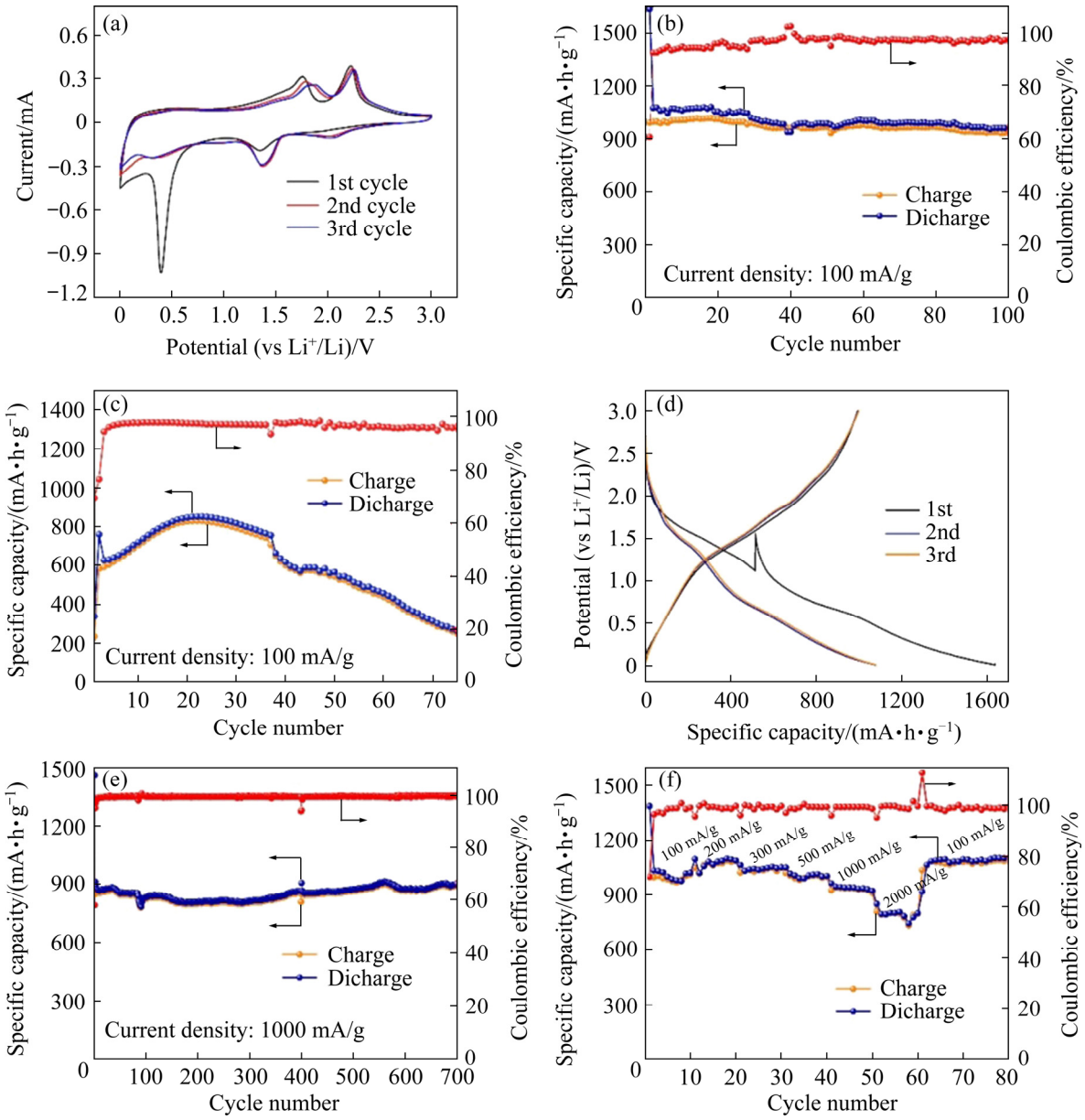

Fig. 5 Electrochemical properties: CV curves of MoS_2/graphene electrode at 0.1 mV/s (a), cycling performance of MoS_2/graphene electrode (b) and pure MoS_2 electrode (c) at 100 mA/g, galvanostatic charge/discharge voltage profiles at 100 mA/g (d), cycling performance at 1000 mA/g (e), and rate performance ranging from 100 to 2000 mA/g (f) of MoS_2/graphene electrode

discharge curve is consistent with the results of CV curve, corresponding to the irreversible transformation reaction of Li_xMoS_2 and the embedding reaction of Li^+, respectively. Meanwhile, the charge capacities of the first three cycles are 845.4, 863.9 and 861.4 mA·h/g, respectively. The well-overlapped curves in the subsequent cycles imply that MoS_2/graphene anode has excellent reversibility. In addition, the MoS_2/graphene anode composite also demonstrates excellent durability under high current density in the long-term cycling tests. Figure 5(e) displays that the cycling stability of MoS_2/graphene nanoflowers anode is 901.8 mA·h/g under a current density of 1000 mA/g over 700 cycles, and the corresponding capacity retention is 98.9% from the 2nd cycle onwards. Except the excellent durability, the MoS_2/graphene anode also demonstrates stable bate performance. As illustrated in Fig. 5(f), the anode also renders high reversible specific capacities of 992, 1067, 1037, 1000, 930, and 788 mA·h/g under the current densities of 100, 200, 300, 500, 1000, and

2000 mA/g, respectively. When the rate comes back to 100 mA/g, a stable specific capacity of 1077 mA·h/g can be recovered. With the increase of current density in the first 20 cycles, the reversible capacity exhibits an upward tendency, attributing to the slow activation of MoS_2. The superior cycling ability is obtained owing to the unique huge nanoflowers structure of MoS_2/graphene composite, which effectively alleviates the pulverizing of nanoparticles for the volume expansion of MoS_2 in the process of charge−discharge.

When the vertical MoS_2 nanosheets are patterned onto graphene as nanoflowers, both cycle life and capacity retention are significantly enhanced, indicating that the nanoflower structures not only improve the electrochemical performance, but also maintain the structural integrity of the electrode, which can be proved by the SEM images before (Fig. 6(a)) and after (Fig. 6(b)) cycling. The images show that most MoS_2/graphene nanocomposites retain their original flower-like shape after 700 cycles under a current density of 1000 mA/g.

Overall, the superior electrochemical performance of the MoS_2/graphene nanoflowers anode is attributed to the few-layered structure of MoS_2 and high conductive graphene. Such unique structures can effectively shorten the solid-state diffusion length for Li^+ owing to the flower-like and nanoscale MoS_2, enhance the electrical conductivity of the whole electrode due to the three-dimensional conducting graphene network, and provide plenty of transmission routes for electrolyte-facilitating diffusion channels of Li^+ within the electrode material. Consequently, the MoS_2/graphene nanoflowers exhibit outstanding reversible capacity, ultrahigh charge−discharge rate properties, and superior cycling performance compared to other nano-sized MoS_2/carbon materials with different structures (Table 1).

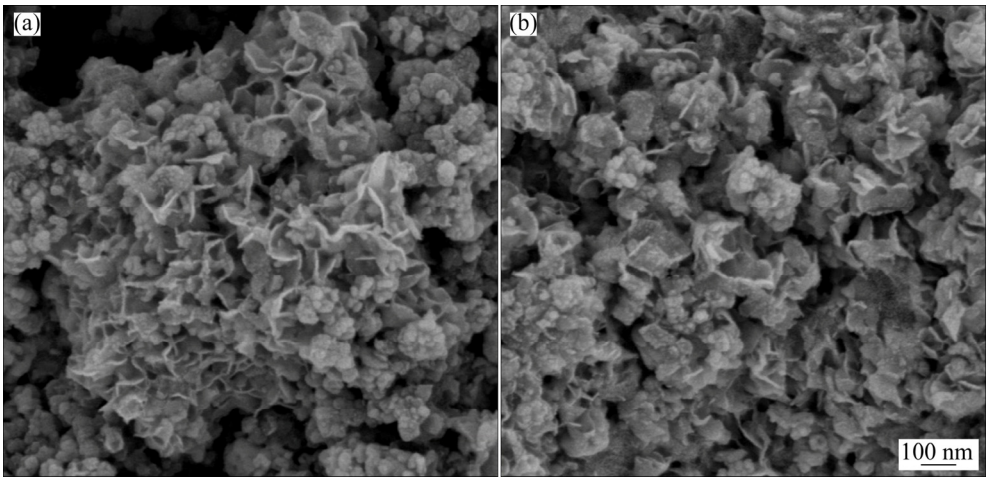

Fig. 6 SEM images of MoS_2/graphene nanocomposite before (a) and after (b) 700 cycles under current density of 1000 mA/g

Table 1 Performance comparison for MoS_2/carbonaceous material with different structures

Material	Structure	Current density/(mA·g^{-1})	Capacity/(mA·h·g^{-1})	Cycle number
MoS_2/graphene (this work)	Nanoflower	100 1000	961 901.8	100 700
MoS_2/C [21]	Microfiber	100	335	100
MoS_2/carbon [22]	Nanourchin	50	721	100
MoS_2/C [23]	2D nanowall	200	880	50
MoS_2/C [24]	2D mesoporous	100	1140	300
MoS_2/RGO [13]	Nanoflower	100 500	1052 800	80 250
MoS_2/graphene [10]	Nanoflower	100 1000	1100 890	60 50

4 Conclusions

(1) The vertically aligned MoS_2 nanosheets were successfully patterned onto graphene substrate to produce 3D MoS_2/graphene nanoflowers through a two-step hydrothermal method.

(2) The unique vertical channels of MoS_2 nanosheets and high conductivity of graphene endow 3D MoS_2/graphene nanoflowers anode with good mechanical and cycling stability.

(3) 3D MoS_2/graphene nanoflowers anode delivered ultrahigh-specific capacities of 961 and 901.8 mA·h/g at and 1000 mA/g, respectively.

(4) Such a 3D hybrid structure design holds great promise for widespread applications such as catalyst and capacitors, and is ready to extend to other 3D sulfides, oxides and nitrides materials.

Acknowledgments

The financial support of the Natural Science Foundation of Changsha, China (No. kq2202094) and National Key R&D Program of China (No. 2021YFB3701400) is greatly appreciated.

References

[1] JI Yi-ru, WENG Su-ting, LI Xin-Yan, ZHANG Qing-hua, GU Lin. Atomic-scale structural evolution of electrode materials in Li-ion batteries: A review[J]. Rare Metals 2020, 39: 205−217.

[2] OAKES L, CARTER R, HANKEN T, COHN A P, SHARE K, SCHMIDT B, PINT C L. Interface strain in vertically stacked two-dimensional heterostructured carbon-MoS_2 nanosheets controls electrochemical reactivity[J]. Nature Communications, 2016, 7: 11796.

[3] LV Qian, LV Rui-tao. Two-dimensional heterostructures based on graphene and transition metal dichalcogenides: Synthesis, transfer and applications [J]. Carbon, 2019, 145: 240−250.

[4] NAGARAJU D H, WANG Q X, BEAUJUGE P, ALSHAREEF H N. Two-dimensional heterostructures of V_2O_5 and reduced graphene oxide as electrodes for high energy density asymmetric supercapacitors [J]. Journal of Materials Chemistry A, 2014, 2: 17146−17152.

[5] ZENG Jing, HUANG Jing-dong, LIU Jun, XIE Tian, PENG Chao-qun, LU Ya-kun, LU Pei-jie, MIN Jie. Self-assembly of single layer V_2O_5 nanoribbon/graphene heterostructures as ultrahigh-performance cathode materials for lithium-ion batteries [J]. Carbon, 2019, 154: 24−32.

[6] ANASORI B, LUKATSKAYA M R, GOGOTSI Y. 2D metal carbides and nitrides (MXenes) for energy storage [J]. Nature Reviews Materials, 2017, 2: 16098.

[7] WANG X F, KAJIYAMA S, IINUMA H, HOSONO E, ORO S, MORIGUCHI I, OKUBO M, YAMADA A. Pseudocapacitance of MXene nanosheets for high-power sodium-ion hybrid capacitors [J]. Nature Communications, 2015, 6: 6544.

[8] XING Lin-shen, LI Xiao, WU Zheng-chen, YU Xue-feng, LIU Ji-wei, WANG Lei, CAI Chen-yuan, YOU Wen-bin, CHEN Guan-yu, DING Jing-jun, CHE Ren-chao. 3D hierarchical local heterojunction of MoS_2/FeS_2 for enhanced microwave absorption [J]. Chemical Engineering Journal, 2020, 379: 122241.

[9] PAN Qi-chang, ZHANG Qiao-bao, ZHENG Feng-hua, LIU Yan-zhen, LI You-peng, OU Xing, XIONG Xun-hui, YANG Cheng-hao, LIU Mei-lin. Construction of MoS_2/C hierarchical tubular heterostructures for high-performance sodium ion batteries [J]. ACS Nano, 2018, 12(12): 12578−12586.

[10] LI Hong-lin, YU Ke, FU Hao, GUO Bang-jun, LEI Xiang, ZHU Zi-qiang. MoS_2/graphene hybrid nanoflowers with enhanced electrochemical performances as anode for lithium-ion batteries [J]. The Journal of Physical Chemistry C, 2015, 119: 7959−7968.

[11] ZHAO Chen-yang, WANG Xu, KONG Jun-hua, ANG Jia-ming, LEE P S, LIU Zhao-lin, LU Xue-hong. Self-assembly-induced alternately stacked single-layer MoS_2 and N-doped graphene: A novel van der Waals heterostructure for lithium-ion batteries [J]. ACS Applied Materials & Interfaces 2016, 8: 2372−2379.

[12] ZHAN Jing, XU Chang-fan, LONG Yi-yu, LI Qi-hou. Preparation and electrochemical performance of nitrogen-doped carbon-coated $Bi_2Mn_4O_{10}$ anode materials for lithium-ion batteries [J]. Transactions of Nonferrous Metals Society of China, 2020, 30: 2188−2199.

[13] XIONG Fang-yu, CAI Zheng-yang, QU Long-bing, ZHANG Peng-fei, YUAN Ze-fang, ASARE O K, XU Wang-wang, LIN Chao, MAI Li-qiang. Three-dimensional crumpled reduced graphene oxide/MoS_2 nanoflowers: A stable anode for lithium-ion batteries [J]. ACS Applied Materials & Interfaces 2015, 7: 12625−12630.

[14] JIANG Lian-fu, LIN Bing-hui, LI Xiao-ming, SONG Xiu-feng, XIA Hui, LI Liang, ZENG Haibo. Monolayer MoS_2-graphene hybrid aerogels with controllable porosity for lithium-ion batteries with high reversible capacity [J]. ACS Applied Materials & Interfaces, 2016, 8: 2680−2687.

[15] WANG Gang, ZHANG Jian, YANG Sheng, WANG Faxing, ZHUANG Xiao-dong, MÜLLEN K, FENG Xin-liang. Vertically aligned MoS_2 nanosheets patterned on electrochemically exfoliated graphene for high-performance lithium and sodium storage [J]. Advanced Energy Materials, 2018, 8: 1702254.

[16] SUN Dan, YE De-lai, LIU Ping, TANG You-gen, GUO Jun, WANG Lian-zhou, WANG Hai-yan. MoS_2/graphene nanosheets from commercial bulky MoS_2 and graphite as anode materials for high rate sodium-ion batteries [J]. Advanced Energy Materials, 2018, 8: 1702383.

[17] HOU Yang, LI Jian-yang, WEN Zhen-hai, CUI Shu-mao, YUAN C, CHEN Jun-hong. N-doped graphene/porous g-C_3N_4 nanosheets supported layered-MoS_2 hybrid as robust anode materials for lithium-ion batteries [J]. Nano Energy, 2014, 8: 157−164.

[18] ZHANG Xiao, ZHANG Qian-wen, SUN Yan-fang, ZHANG Peng-yun, GAO Xue, ZHANG Wen, GUO Jin-wen. MoS_2-graphene hybrid nanosheets constructed 3D architectures with improved electrochemical performance for lithium-ion batteries and hydrogen evolution [J]. Electrochimica Acta, 2016, 189: 224−230.

[19] YANG Qian, LIANG Qiang, LIU Jun, LIANG Shu-quan, TANG Sha-sha, LU Pei-jie, LU Yakun. Ultrafine MoO_2 nanoparticles grown on graphene sheets as anode materials for lithium-ion batteries [J]. Materials Letters, 2014, 127: 32−35.

[20] SANTHOSHA A L, NAYAK P K, POLLOK K, LANGENHORST F, ADELHELM P. Exfoliated MoS_2 as electrode for all-solid-state rechargeable lithium-ion batteries [J]. The Journal of Physical Chemistry C, 2019, 123(19): 12126−12134.

[21] VALDEZ A, VILLARREAL J, ZUNIGA L, ALCOUTLABI M. MoS_2 and MoO_2 loaded carbon microfibers as anode materials for lithium-ion and sodium-ion batteries [J]. ECS Transactions, 2018, 85(13): 357−368.

[22] WANG Qiang, LI Jing-hong. Facilitated lithium storage in MoS_2 overlayers supported on coaxial carbon nanotubes [J]. The Journal of Physical Chemistry C, 2007, 111: 1675−1682.

[23] XIAO Jie, WANG Xiao-jian, YANG Xiao-qing, XUN Shi-di, LIU Gao, KOECH P K, LIU Jun, LEMMON J P. Electrochemically induced high capacity displacement reaction of PEO/MoS_2/graphene nanocomposites with lithium [J]. Advanced Functional Materials, 2011, 21: 2840−2846.

[24] FANG Yin, LV Ying-ying, GONG Feng, ELZATAHRY A A, ZHENG Geng-feng, ZHAO Dong-yuan. Synthesis of 2D-mesoporous-carbon/MoS_2 heterostructures with well-defined interfaces for high-performance lithium-ion batteries [J]. Advanced Materials, 2016, 28: 9385−9390.

先进锂离子电池用三维纳米花状 MoS_2/石墨阳极

何汉兵[1]，刘 真[1]，彭超群[2]，刘 军[2]，王小锋[2]，曾 婧[1]

1. 中南大学 冶金与环境学院，长沙 410083；
2. 中南大学 材料科学与工程学院，长沙 410083

摘 要：采用两步水热合成法将垂直的二硫化钼(MoS_2)纳米片可控地负载于石墨烯表面形成纳米花。二硫化钼纳米片和石墨烯形成紧密结合的垂直交互网络结构，使电极具有高的机械完整性和循环稳定性。所得 MoS_2/石墨烯纳米花阳极在 1000 mA/g 电流密度下稳定循环 700 次后，仍具有 901.8 mA·h/g 的超高比容量，且从第二次循环开始，相应的容量保持率为 98.9%。

关键词：二硫化钼；石墨烯；三维纳米花；纳米片；锂离子电池

(Edited by Xiang-qun LI)